Journal of Magnetism and Magnetic Materials 465 (2018) 309–315

Contents lists available at ScienceDirect

Journal of Magnetism and Magnetic Materials

journal homepage: www.elsevier.com/locate/jmmm

Research articles

Structural, optical, dielectric and magnetic properties of $Bi_{1-x}La_xFeO_3$ nanoparticles

E.K. Abdel-Khalek[a,*], Islam Ibrahim[b], Tarek M. Salama[b,*], Ahmed M. Elseman[c], Mohamed Mokhtar Mohamed[d]

[a] Department of Physics, Faculty of Science, Al Azhar University, Nasr City11884, Cairo, Egypt
[b] Department of Chemistry, Faculty of Science, Al-Azhar University, Nasr City 11884, Cairo, Egypt
[c] Central Metallurgical Research & Development Institute (CMRDI), P.O. Box 87, 11421 Cairo, Egypt
[d] Department of Chemistry, Faculty of Science, Benha University, Benha, Egypt

ARTICLE INFO

Keywords:
Nanoparticles
Rietveld refinement
Optical properties
Dielectric materials
Magnetic properties
Exchange bias effect

ABSTRACT

In this work, the structural, optical, dielectric and magnetic properties of $Bi_{1-x}La_xFeO_3$ nanoparticles (x = 0.50 and 0.75) have been investigated at room temperature. Structural analysis indicated the coexistence of orthorhombic (Pbnm) and rhombohedral (R3c) phases. UV–visible absorption spectra of the samples exhibit two doubly degenerate d-d transitions and three charge transfer transitions. Using diffused reflectance UV–Vis spectra, the direct and indirect band gaps of the samples decreases with increasing La content. The dielectric constant (ε) of the samples in the microwave region exhibited an anomalous phenomenon at room temperature. Magnetic hysteresis loops (M − H) of the samples exhibit weak ferromagnetism and an antiferromagnetic order. Additionally, the exchange bias effect was observed in these samples at room temperature. These results demonstrate that the method presented may be considered an effective way to improve the magnetic and optical properties of $Bi_{1-x}La_xFeO_3$.

1. Introduction

Recently, $Bi_{1-x}La_xFeO_3$ nanoparticle materials have attracted much attention because of their unique structural, optical, electric and magnetic properties [1–4]. These properties are owing to the simultaneous existence of electric and magnetic (ferromagnetic and/or antiferromagnetic) ordering [1–4]. Additionally, these properties are due to also the magnetoelectric coupling between the ferroelectric and magnetic order parameters (charge and spin) [2,4]. These unique properties lead to manifold possible applications such as novel magnetoelectric devices, memories, sensors, visible light photocatalytic activity, etc. [1–4]. It is known that the structural phase diagram of $Bi_{1-x}La_xFeO_3$ at room temperature is one of the most controversial aspects [5,6]. Recent studies showed that the most interesting feature of the crystal structure is the coexistence of orthorhombic and rhombohedral phases in $Bi_{1-x}La_xFeO_3$ [5–7].

Khodabakhsh et al. [8] investigated the phase transition temperatures of sol-gel synthesized $Bi_{1-x}La_xFeO_3$ ($0.05 \le x \le 0.15$) powders. They found that the coexistence of rhombohedral (R3c) and orthorhombic (pbnm) phases from the Rietveld analysis. Suresh and Srinath [9] investigated the structure and magnetic properties of $Bi_{1-x}La_xFeO_3$ ($0.05 \le x \le 0.4$) samples. The refinement results show the coexistence of rhombohedral (R3c) and orthorhombic (pbnm) phases in this range [9]. Quinonez et al. [10] investigated the UV–Vis absorption spectra for $BiFeO_3$ nanoparticles collected by diffuse reflectance. They found that the $BiFeO_3$ sample exhibits both direct and indirect band gaps. Li et al. [11] investigated the dielectric properties of La doped $BiFeO_3$ in the microwave region. They found that the La doped $BiFeO_3$ samples exhibit featured frequency response which effected by the amount of doping, distorted structure and defects. Mazumder et al. [12] investigated the magnetic properties of pure and doped $BiFeO_3$ samples. They found that these samples exhibit weak magnetization and an antiferromagnetic order. Additionally, the magnetic hysteresis loops exhibit exchange bias effect.

Unfortunately, the spontaneous polarization and magnetization of $BiFeO_3$ samples at room temperature (RT) have small values [2]. These values are due to the presence of secondary non-perovskite phases such as $Bi_2Fe_4O_9$, $Bi_{25}FeO_{40}$ and Bi_2O_3/Fe_2O_3 and high leakage current which is due the presence of Fe^{2+} ions [2,13]. Recently to address these problems and to improve the properties of $BiFeO_3$, some efforts have focused on the synthesized method and the substitution of Bi by La ions [14]. To the best of our knowledge there are very few reports to study

* Corresponding authors.
E-mail address: Eid_khalaf1@yahoo.com (E.K. Abdel-Khalek).

https://doi.org/10.1016/j.jmmm.2018.06.024
Received 10 April 2018; Received in revised form 4 June 2018; Accepted 10 June 2018

the dielectric properties of $Bi_{1-x}La_xFeO_3$ in the microwave region. In spite of the magnetoelectric devices are operating in the microwave region [15]. Additionally, there are still a lot of controversies about the electric origin of $Bi_{1-x}La_xFeO_3$ in the coexistence of orthorhombic and rhombohedral phases [5]. In view of the aforementioned aspects, we fabricate $Bi_{1-x}La_xFeO_3$ (x = 0.50 and 0.75) nanoparticles by novel hydrothermal-assisted co-precipitation method. In this study, the structural, optical, dielectric in the microwave region (1 MHz–3 GHz) and magnetic properties of $Bi_{1-x}La_xFeO_3$ at room temperature have been investigated.

2. Experimental

2.1. Samples preparation

$Bi_{1-x}La_xFeO_3$ (x = 0.50 and 0.75) perovskites were prepared by using hydrothermal assisted co-precipitation method which is used to prepare nanoparticles with high performance at relatively low temperature. First step, $Fe(NO_3)_3{\cdot}9H_2O$, $Bi(NO_3)_3{\cdot}5H_2O$ and $LaCl_3{\cdot}7H_2O$ salts were dissolved in distilled water. Metal nitrate solutions were mixed in appropriate proportions depending on the target composition. The cations were coprecipitated by dropwise addition of a certain amount of saturated aqueous solution of $(NH_4)_2CO_3$. The solution was heated with stirring using hot plate with magnetic stirrer. Second step, hydrothermal treatment, the precipitate solution was transferred to a sealed Teflon-lined stainless steel autoclave and annealed at 180 °C for 48 h. The obtained products were filtered and washed with hot distilled water. A few grams of the obtained powders were then pressed into pellets that were sintered at 1173 K for 12 h in air to obtain a highly dense final product.

2.2. Samples characterization

X-ray diffraction (XRD) patterns of the samples at room temperature were obtained from SIEMENS D5000 diffractometer with Cu K_α radiation. The structural refinements were carried out using the FULLPROF Rietveld program. The average particle sizes and morphology of all the samples were directly imaged by transmission electron microscopic (TEM) utilizing a JEOL JEM-1010 microscope. The Fourier transform infrared (FTIR) spectra of the samples were recorded in the range of 400–850 cm^{-1} by a JASCO FT/IR-430 spectrophotometer with a resolution of 2 cm^{-1} using KBr pellets. The optical absorption spectra of the samples were recorded in the spectral range 0.56–5.5 eV by a Jasco 570 UV–VIS-NIR spectrophotometer. Dielectric studies were carried out using an Hioki 3532-50LCR Hitester as a function of frequency (1 MHz–3 GHz). The magnetic hysteresis loops were recorded at RT using vibrating sample magnetometer (VSM), 7410 Lakeshore USA, in maximum applied field of 20 kG.

3. Results and discussion

3.1. XRD and TEM studies

Fig. 1 shows the observed and fitted XRD patterns of $Bi_{1-x}La_xFeO_3$ (x = 0.50 and 0.75) samples. It is important to note that the XRD patterns of the present samples show two phases without the foreign non-perovskite phases of $Bi_2Fe_4O_9$, $Bi_{25}FeO_{40}$ and Bi_2O_3/Fe_2O_3, although they are observed in some previous studies [16,17]. The Rietveld refinement of the samples was carried out for orthorhombic (Pbnm space group) with Wyckoff position of Bi/La at 4c, Fe at 4a, O1 at 4c and O2 at 8d and rhombohedral (R3c space group) with Wyckoff position of Bi/La and Fe at 6a and O at 18b [18,19]. The refined values of the lattice parameters, unit cell volume, phase fraction, positional coordinates and R-factors are listed in Table 1. It is evident from this table that the crystal structure for the x = 0.50 sample is characterized by a dominant orthorhombic phase (90.24%) with a minor rhombohedral phase

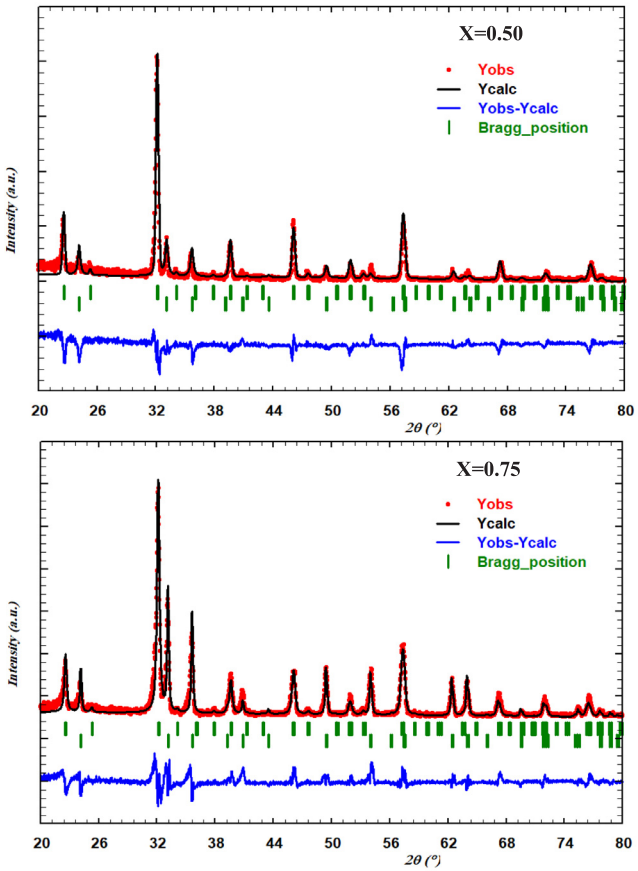

Fig. 1. Rietveld plot of X-ray diffraction pattern for $Bi_{1-x}La_xFeO_3$ samples as a function of the x mol%. Red dots indicate the experimental date and black lines overlapping them indicate calculated profiles. The lowest curve shows the difference between experimental and calculated patterns. Bragg positions assigned to the orthorhombic and rhombohedral phases are marked by vertical ticks, respectively. (For interpretation of the references to colour in this figure legend, the reader is referred to the web version of this article.)

(9.76%) [16,20]. This is consistent with the previous reports [9,21]. The amount of rhombohedral phase increases with increasing La upto x = 0.75 on expense of Bi which means the decrease in the structural distortion [16,18]. From Table 1, it is noticed that the lattice parameters and unit cell volumes increase with increasing La upto x = 0.75 which due to the lowering of the oxygen vacancies concentration because of the lower strength of Bi–O (343 kJ mol^{-1}) relative to that of La–O (799 kJ mol^{-1}) [5].

Fig. 2 shows the TEM images of the $Bi_{1-x}La_xFeO_3$ (x = 0.50 and 0.75) samples. From TEM images, the particle shapes are nearly spherical besides showing some agglomerated and irregularly shaped particles [22–24]. The presence of agglomerated particles may be attributed to the high surface energy of small-sized particles [25]. These images also reveal changes in shape and size of particles with increasing La on expense of Bi due to the changes in structural anisotropy of the nanoparticles as well as the transformation from orthorhombic to rhombohedral geometry [26,27]. The particle sizes distributions (PSD) of the $Bi_{1-x}La_xFeO_3$ (x = 0.50 and 0.75) samples are shown in the inset of Fig. 2. The average particle sizes are found to be 20.48 and 32.06 for x = 0.50 and 0.75, respectively. The average particle sizes increase with increasing La upto x = 0.75 can be attributed to the partial structural transformation from orthorhombic to rhombohedral and the increase of lattice parameters [18,28].